Received: 22 March 2024 | Revised: 31 July 2024 | Accepted: 8 November 2024 | Published online: 14 November 2024

RESEARCH ARTICLE

Design and Demonstration of a Novel Interferometric Polarimeter for Quantitative Determination of Sugars in a Solution

Journal of Optics and Photonics Research
2024, Vol. XX(XX) 1–14
DOI: 10.47852/bonviewJOPR42022890

BON VIEW PUBLISHING

Rahim Ullah[1,*], Raheem Dad Khan[2], Ghazanfar Hussain[1], Rahat Ullah[1] and Muhammad Faisal[1,*]

[1]*National Institute of Lasers and Optronics College, Pakistan Institute of Engineering and Applied Sciences, Pakistan*
[2]*Department of Physics and Applied Mathematics, Pakistan Institute of Engineering and Applied Sciences, Pakistan*

***Corresponding authors**: Rahim Ullah, National Institute of Lasers and Optronics College, Pakistan Institute of Engineering and Applied Sciences, Pakistan. Email: rahimullahphysics28@gmail.com and Muhammad Faisal, National Institute of Lasers and Optronics College, Pakistan Institute of Engineering and Applied Sciences, Pakistan. Email: mfaisal13@yahoo.com

Abstract: Accurate quantification of sugar in food and pharmaceutical products is important to achieve the desired levels of sweetness, texture, flavor and nutritional content. This article introduces a novel polarization-sensitive interferometric method for measuring the concentration of sugar in solutions. The impact of sugar concentration is investigated by analyzing the visibility of the interference pattern using a Mach-Zehnder interferometer with an interference pattern scanning and recording system. The visibility of the interference fringes is determined by cross-sectional scanning of the fringe pattern from its center over the photodetector, followed by cut-profile analysis. As the concentration of sucrose, glucose and fructose increases, a gradual decrease in interference pattern visibility is observed, following a parabolic trend within the broader detection range of 0–14 g/50 ml. The sensor's performance is divided into two linear regions: region-1 (0–6 g/50 ml) and region-2 (6–14 g/50 ml). In region-1, fructose exhibited the highest sensitivity of 0.0195 $(g/50\ ml)^{-1}$, which is 6.09 times and 1.89 times higher than glucose and sucrose, respectively. Similarly, in region-2, fructose showed a sensitivity of 0.077 $(g/50\ ml)^{-1}$, surpassing glucose by 3.56 times and sucrose by 2.41 times. However, sucrose achieved the lowest limit of detection of 0.0021 g/ml, which is 2.76 times and 1.71 times better than glucose and fructose, respectively. The decreasing trend in interference pattern visibility is further validated through irradiance and optical rotation measurements of the laser beam passing through the sugar solutions relative to the reference laser beam. Results from both optical techniques demonstrated good agreement, with average deviations of 1.75%, 1.72%, and 4.24% for sucrose, glucose and fructose, respectively. The proposed technique is universally applicable for measuring the concentration of transparent, optically active solutions and has the potential to be a valuable tool for quality control and optimization in the food and pharmaceutical industries.

Keywords: optical interferometry, optical rotation, sugar, optically active material, interference pattern visibility

1. Introduction

Quantification of saccharides in different solutions is pivotal for various applications, including standardized food and beverages production, pharmaceuticals, biotechnology and medical research [1]. Saccharides are essential components in a multitude of products and processes, such as sweetening products and intensifying flavor [2, 3], stabilizing active ingredients and improving the solubility of drugs in pharmaceuticals [4-7] and providing an appropriate environment for cells or organisms to proliferate and function in biotechnology researches [8-10]. Moreover, sugar concentration in the blood or other bodily fluids can

be utilized to diagnose and monitor diseases, specifically diabetes [11-16]. Quantifying sugar in solutions is also imperative for guaranteeing food product quality and safety, allowing manufacturers to meet desired specifications and yield safe products for consumption, since higher levels of sugar in the blood can increase the risk of diabetes, obesity, heart diseases and accelerate aging [17].

Concentration measurement of chiral materials is often remained the subject of biochemical analysis. Various other reported techniques include refractometery [18], microgap biosensing [19], spectrometry [20], Fourier transform near-infrared spectroscopy (FT-NIR) [21], attenuated total reflectance terahertz (ATR-THz) spectroscopy [22, 23], conductivity variation with varying radiofrequency [24], terahertz nano-antennas [25], microwave cavity perturbation [26], etc. Sugar detection using optical techniques are particularly appealing for several reasons: they are fast, immune to electromagnetic interference, remotely measurable, utilize non-ionizing radiation for interrogation of the sample and generally do not require consumable reagents [27]. Optical detection include holography [28, 29], optical nanoprobes [30], speckle decorrelation [31], polarized Muller's matrices [32], Bragg diffraction [33], polarimetry [34-37], interferometry [38], etc.

Saccharides, being chiral or optically active carbohydrates, have been subjected to polarimetry for decades as a well-known optical detection technique for the quantitative analysis of sugar [39-43]. It determines a rotation of the angle of polarization when a polarized light passes through their solutions. The magnitude of the angle of rotation is distinct for different materials at different concentrations, thus allowing for the estimation of their concentrations from the degree of rotation in the plane of polarization of a laser beam that passes through their solutions [44]. Chiral materials are typically composed of at least one asymmetric atom in their molecular structure, such as carbon, sulfur, phosphorus, and silicon. This asymmetry results in the formation of two different types of isomers. The isomer that rotates the plane of polarization clockwise is known as dextrorotatory or right-handed, while the isomer that results in the anticlockwise rotation of the polarization is called levorotatory or left-handed. Although the geometrical shape and chemical composition of both molecules are identical, they are mirror images of each other and are referred to as enantiomers. Both enantiomorphs rotate the plane of polarization of light by the same magnitude, but in opposite directions. Biot's law describes the mathematical equation for the optical interaction of linearly polarized light with chiral specimens as:

$$[\alpha]_{\lambda}^{T} = \frac{\alpha}{LC} \tag{1}$$

The term $[\alpha]_{\lambda}^{T}$ is known as specific rotation of the chiral material when exposed to a specific wavelength of light (λ) at temperature (T), where, α is the rotation of the plane of polarization of the transmitted light, L is the optical path-length in the sample and C is its concentration.

Optical interferometry is an efficient optical technique utilized to quantitatively assess chiral samples in solution [45-52]. The quantitative determination can be performed by measuring visibility of the interference pattern [53]. Generally, a polarized laser beam is divided into two parts, one of which is transmitted through the chiral solution and is then interfered with the other part of the laser beam. Chiral materials rotate the plane of polarization of the light beam according to their concentration which directly affects the visibility of interference, and causes a proportional incoherence in the sensing beam of the interferometer. Interference pattern contrast is ideally one when both reference and sample beams have perpendicular polarization to the plane of incidence and have the same intensities. However, the interference vanishes and hence the visibility becomes zero when polarization of the sample and reference light-beams are perpendicular to each other, even with same intensity of the two light beams. The visibility of the interference pattern is determined from the interference pattern as [38]:

$$V = \frac{I_{max} - I_{min}}{I_{max} + I_{min}} \tag{2}$$

Where, V is the visibility, I_{max} and I_{min} represent the resultant irradiances corresponding to maxima and adjacent minima in the interference pattern. By determining the polarimetric measurement of the laser beam passing through the chiral sample, visibility can also be defined as,

$$V = \frac{2\sqrt{I_1 I_2}}{I_1 + I_2} cos\theta \tag{3}$$

Where, I_1 and I_2 are the irradiances of reference and sample beams respectively and θ is rotation of the polarization vector of the sample beam [38]. The intensity of light absorbed by a solution is directly proportional to its concentration, which can be quantified using by Beer-Lambert's law [54];

$$A = \alpha(\lambda) LC \tag{4}$$

Where A represents the absorbance, $\alpha(\lambda)$ denotes the wavelength dependent absorption coefficient, L and C show the optical path length in the sample and the concentration of the solution respectively. In the literature, the interference patterns are typically evaluated through image processing, which necessitates a high-quality CCD or CMOS camera to capture images of the

interference pattern at varying concentrations of chiral solutions, the visibility of which is then determined through image processing [38, 55]. This analytical technique is prone to speckle noise, which limits the detection capability of the device.

This article presents a novel, to the best of our knowledge, polarization-sensitive interferometric approach for quantitatively measuring the concentration of chiral materials such as sucrose, glucose and fructose in a solution. A sample tube containing the sugar sample of a specific concentration is placed in one arm of a Mach-Zehnder interferometer, and the resulting interference patterns are scanned onto a photodetector to record the interference pattern in real-time. The visibility of the interference pattern is determined as a function of concentration of sugar, with a decrease in the visibility of the pattern observed with an increase in the concentration of the sugar sample due to incoherence caused by the sugar solution when the polarized laser beam passes through it. Visibilities of interference patterns are cross-varified by measuring the optical rotation in the plane of polarization and irradiance of the transmitted beam through the sample using Equation 3. The reported technique can be applied to determine the concentration of any transparent optically active solutions.

2. Experimental Setup

The designed interferometric-polarimeter composed of Mach-Zehnder interferometer and interference pattern scanning and recording system. Laser beam from a stabilized HeNe laser (wavelength: 632.8 nm, output power: 1 mW, beam diameter: 1 mm, vertically polarized) is guided by an aluminum coated mirror M_1 towards a Faraday isolator to prevent back-reflections in the laser. The transmitted laser beam is then divided by a non-polarizing 50:50 beamsplitter BS_1 into two beams, referred to as the reference and sensing beams. These beams are then reflected by two aluminum-coated mirrors (M_2 and M_3) at 90° each. Both the beams are then recombined and interfered at second beamsplitter BS_2. The resultant interference pattern is 30 times magnified by the lenses $L_1$and L_2 and then scanned onto an amplified photodetector module (BPX65) by mirror M_4 driven by a DC servomotor (2.19 arc-sec step, Thorlabs Inc., US) interfaced with a personal computer (PC). The response of the photodetector is then recorded by a digital oscilloscope (1 GHz, 4GSa/s, Agilent Technologies, US) and analyzed by a PC connected to it. The image of the reflected interference pattern from the beamsplitter is also captured by a reflex camera for visual inspection of the interference pattern. Analytical grade D(+)-Sucrose (Applichem), D(+)-Glucose (Chem-Lab), and D(-)-Fructose (VWR Chemical, BDH) are accurately weighed on an electronic balance (AND CB-300) and added to 50 ml of deionized (DI) water. The mixture is stirred at room temperature for 10 minutes on a magnetic hot-plate (Heidolph MR 2002) using a magnetic stirrer. A sample tube (Pyrex glass, internal diameter: 25 mm, length: 146 mm) with anti-reflection (AR)-coated NBK7 windows at the end faces is filled with the sugar solutions and placed in the mid of the sensing arm of the Mach-Zehnder interferometer. The AR-coated NBK7 windows are used to reduce interference artifacts due to reflection and to preserve the polarization state of the integrating laser beam with the sample solution. The arm-lengths of the interferometer are kept about 300 mm and the sample tube is placed at the center of the sensing arm, as schematically shown in Figure 1. The windows of the sample tube are cleaned each time before filling with the solutions. Interference patterns are recorded and analyzed for each solution at different concentrations. The experiment is repeated five times for each concentration, and the results are averaged.

Figure 1

Schematic diagram of the experimental setup for interference fringes scan interferometric- polarimeter. The labels M_1, M_2, M_3 and M_4 represent aluminum coated reflecting mirrors, BS_1 and BS_2 are the nonpolarizing (50:50) beam splitters and L_1 and L_2 are the convex lenses

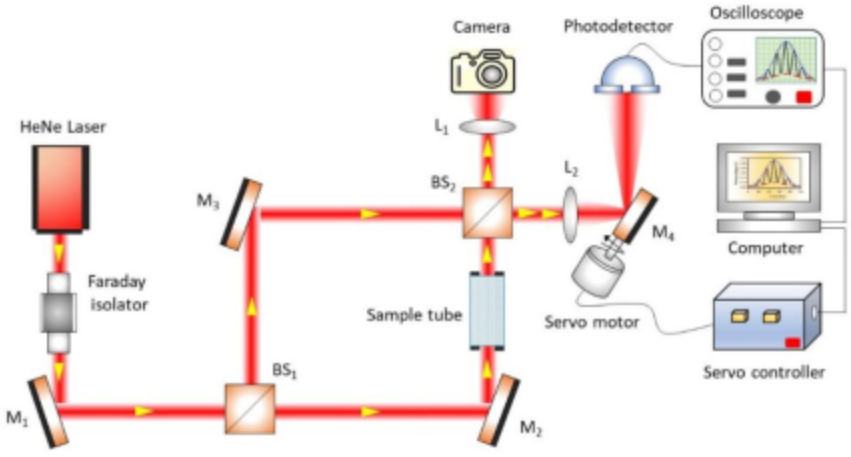

3. Results and Discussion

Subsequent to thorough cleansing, the sample tube was filled with the sugar solutions prepared in DI water. The irradiance and optical rotation of the transmitted laser beam from the sample tube are the primary factors influencing the visibility of the interference fringes. Therefore, both of these parameters were measured one by one for the transmitted beam. Intensity of the transmitted beam was measured by 3Σ laser power energy meter with OP-2 VIS optical sensor head (Coherrent, US). A linear decrease in the transmitted power of the laser beam was observed with an increase of sugar concentration in the solution, as illustrated by the linear fitting over the scatters by solid lines in Figure 2(a). This linear variation in the power of the transmitted beam with the variation in the sugar concentration in the solution can also be confirmed by Beer-Lambert's law, as expressed in Equation 4. Fructose solutions exhibited an absorption of 4.02 μW/(g/50 ml), which was 2.15 and 2.95 times higher than the corresponding sucrose and glucose concentration, respectively. This may be attributed to the light yellowish colour of the fructose solution, which caused a relatively higher absorption. Polarimetric analysis of the sample beam was performed for different sugar solutions by a phase lock-in rotating analyzer (PLRA) polarimeter as reported in our previous paper [44]. DI water showed no optical rotation however, a linear dextrorotatory nature was observed for sucrose and glucose from their positive slopes, and a levorotatory nature was observed for fructose from their negative slope, as shown in Figure 2(b). Fructose displayed a linear variation of -5.46°/(g/50 ml), which was 1.67 and 2.24 times higher than the corresponding magnitudes of opticalrotations of sucrose and glucose, respectively.

Figure 2

(a) Intensity variation of the sample beam after passing through the sample tube with different concentration of sugar solutions. (b) Optical rotation in the polarization of the sample beam caused by the sugar solutions at different concentrations. Solid lines over the corresponding scatters show the linear curve fitting

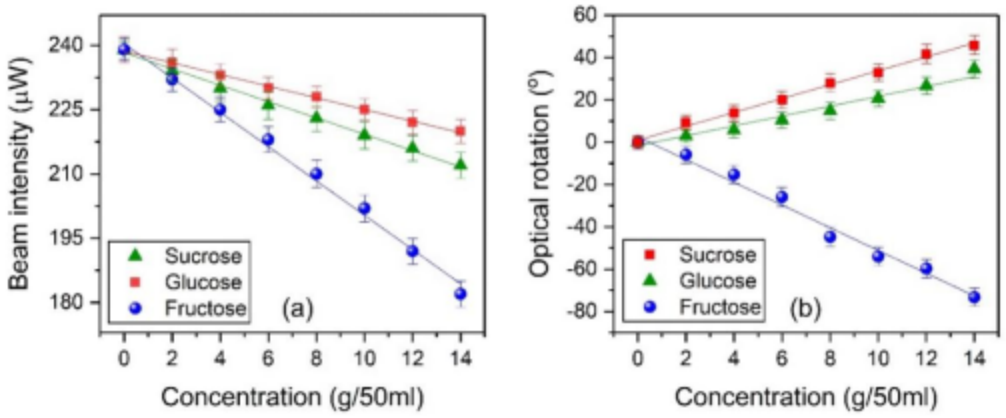

The Cut Profile Analysis is applied for visibility determination of the interference pattern. The interference pattern for each concentration is cross-sectionally scanned from its center over the photodetector, which has a square active area of 1x1 mm. By examining the intensity variations along this 1x1 mm cross-sectional slice, the visibility of the fringes is determined using equation 2 of the manuscript. This approach provides a real-time localized measurement of visibility across the central cross-section of the interference pattern. The central position of the interference pattern is critical to find in distilled water at zero concentration of sugar. Therefore, the interference pattern is vertically scanned across the central fringe, and the position of maximum intensity is fixed to nominate it as the center of the interference pattern.

To prevent distortion of the fringes, the sugar solution in the sample tube was allowed to settle for 3-5 minutes prior to recording the interference pattern. The mirror M_4 was driven by a DC servomotor to scan the interference patterns over the photodetector. The digital oscilloscope then captured the patterns, which are illustrated in Figure 3(a) and 3(b) for deionized water and 14 g/50 ml of sucrose solution, respectively. The central fringes of the interference pattern exhibit the highest intensity, which then decreases in a sequential manner towards the edges. The maxima and minima of each interference pattern are fitted with a Gaussian function, represented by dotted and dashed lines respectively, as shown below;

$$y = y_o + \frac{A e^{\frac{-4\ln(2)(x-x_c)^2}{\Delta w^2}}}{\Delta w\sqrt{\pi/4\ln(2)}} \qquad (5)$$

Where, y_o, A, x_c and Δw are the constants of the function, which define the base, magnitude, center and FWHM of the Gaussian function, respectively. It is evident that the maxima and minima of the interference patterns are accurately traced by the

fitting functions, indicating the perfection of the patterns. The visibility of the interference patterns for DI water and 14 g/ml of sucrose solution was 0.974 and 0.653,respectively. Alongside, the representative optical rotation of DI water and 14 g/50 ml of sucrosesolution are depicted in Figure 3(c) and 3(d). Furthermore, the deterioration in the interference pattern is clearly visible in the photograph taken by the reflex camera for 14 g/ml of sucrose solution as depictedin Figure 3(e). Conversely, DI water showed no deterioration in the interference pattern, as shown in Figure 3(f).

Figure 3
Intensity profile of interference patterns recorded for (a) DI water (b) 14 g/50 ml of sucrose solution. Optical rotation observed by PLRA polarimeter for (c) DI water (d) 14 g/50 ml of sucrose solution. Images of interference patterns captured by reflex camera for (e) DI water and (f) 14 g/50 ml of sucrose solution

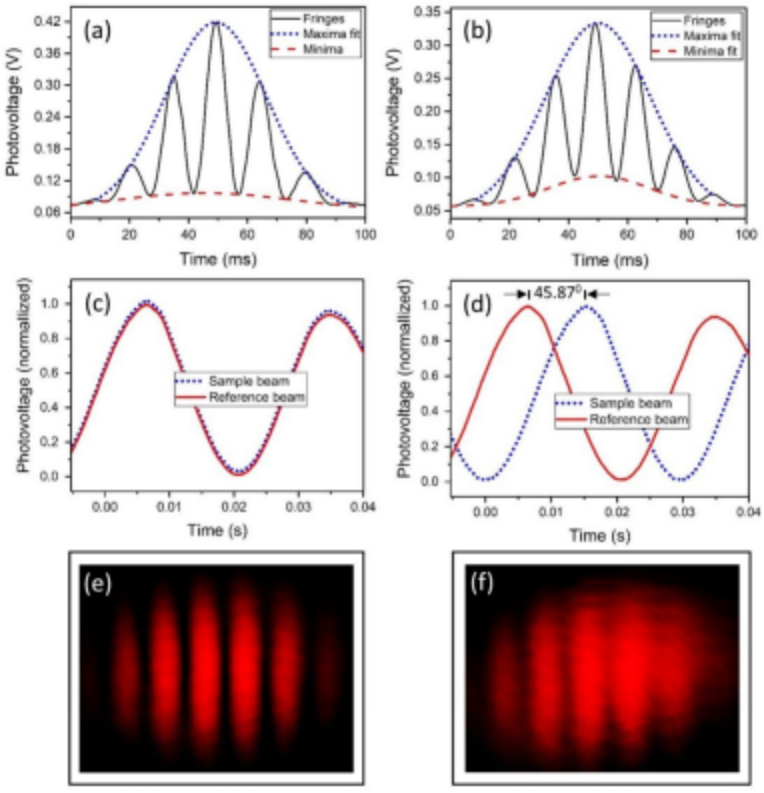

Interference patterns were individually recorded for sucrose, glucose, and fructose at differentconcentrations ranging from 0 to 14 g/50 ml. The visibilities of the corresponding interference patterns were assessed from the maxima and adjacent minima using Equation 2. A sequential decreasing trend is observed in the visibility with increase in the concentration for each sugar sample. To verify the results, visibilities were also calculated from irradiance and optical rotation of the transmitted laser beam from the sugar solutions using Equation 3. For comparison, the detected and calculated visibilities were plotted over each other, as shown in Figure 4. It can be observed that the visibilities detected directly from the interference pattern and those calculated indirectly from the irradiance and opticalrotation followed a similar trend, with an average deviation of 1.75%, 1.72%, and 4.24%, respectively, for sucrose, glucose and fructose. Thus, the performance of the novel polarization-sensitive interferometric scheme was cross-checked and found to be satisfactory. The deterioration of interference fringe visibility for fructose solutions was found to be 1.19 and 128 times greater than that of sucrose and glucose, respectively. This may be associated with the higher optical rotation of fructose solutions, as evidenced by its specific rotation ($[\alpha]_{\lambda}^{T}$) of -92.4 deg dm^{-1} cm^{3} g^{-1} for the D-line of the sodium lamp (λ=589.3 nm, T=20 °C) [56], compared to 66.5 and 52.5 deg dm^{-1} cm^{3} g^{-1} for sucrose and glucose, respectively. Moreover, the absorption of the HeNe laser beam is higher for fructose than for sucrose and glucose, resulting in a lower fringe contrast for fructose solutions. The decreasing trend in the visibilities of interference patterns for glucose and fructose reported by Calixto et al. [38] was supported by a polynomial fitting function of degree 4, which shows the higher degree of nonlinearity in their system which leads to deviation from the theoretical justification in Equation 2 and Equation 3. In comparison, our experimental technique is more cost-effective and does not suffer from speckle noise associated with images taken by a camera, resulting in results that are more closely aligned with the theoretical trend. Furthermore, the rise time of our photodetector (12 ns) is rapid

enough to detect changes in the visibility of the interference pattern quickly. Performance of the designed interferometric polarimeter for three different sugar solutions is summarized in Table 1.

Figure 4
Variations in visibilities with change in sugar concentration as determined from maxima and adjacent minima of the interference patterns using Equation 2, and calculated based on polarimetric rotation and intensity of the transmitted beam through the sugar sample using Equation 3

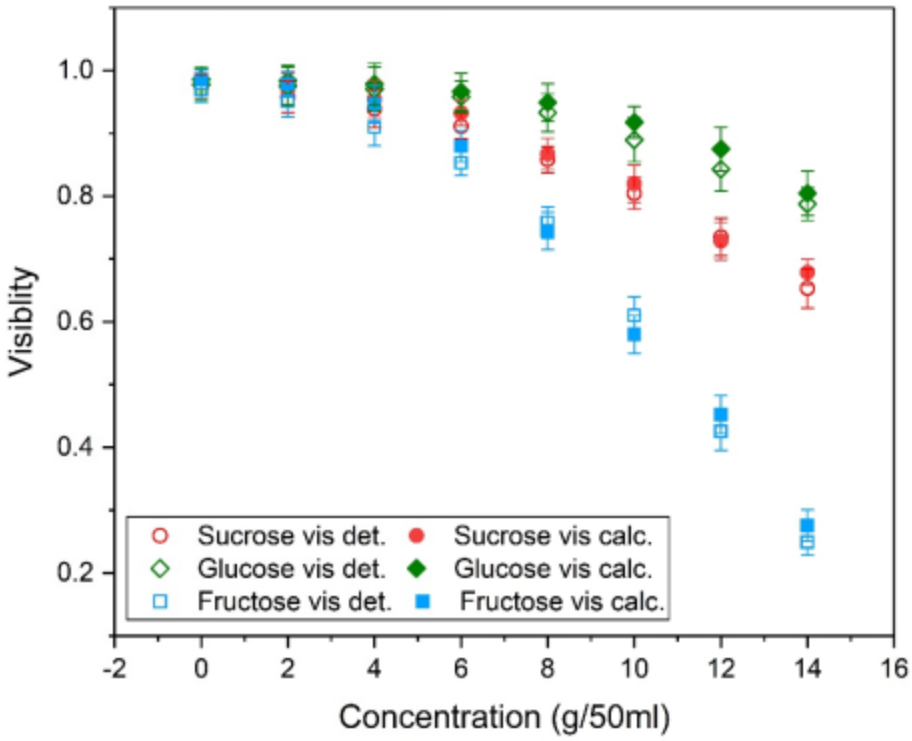

Table 1
Performance summery of the developed interferometric polarimeter for quantification of sugar solutions

Concentration (g/50 ml)		Transmittance (μW)	Optical rotation (°)	Visibility detected	Visibility calculated	Visibility difference (%)
Sucrose	0	239	0	0.97	0.99	1.24
	2	234	9.3	0.96	0.97	1.36
	4	230	13.8	0.94	0.95	1.60
	6	226	19.94	0.91	0.93	2.28
	8	223	28.05	0.86	0.87	1.03
	10	219	33.03	0.80	0.82	1.86
	12	216	41.74	0.74	0.73	0.88
	14	212	45.87	0.65	0.68	3.72

Concentration (g/50 ml)		Transmittance (μW)	Optical rotation (°)	Visibility detected	Visibility calculated	Visibility difference (%)
Glucose	0	239	0	0.98	0.99	0.80
	2	236	2.97	0.98	0.98	0.81
	4	233	5.82	0.97	0.98	0.81
	6	230	10.52	0.96	0.97	0.82
	8	228	14.85	0.93	0.95	1.68
	10	225	20.64	0.89	0.92	3.04
	12	222	26.66	0.84	0.88	3.68
	14	220	34.7	0.79	0.80	2.10
Concentration (g/50 ml)		Transmittance (μW)	Optical rotation (°)	Visibility detected	Visibility calculated	Visibility difference (%)
Fructose	0	239	0	0.97	0.99	1.71
	2	232	-5.86	0.95	0.98	2.74
	4	225	-15.25	0.91	0.95	3.81
	6	218	-25.85	0.85	0.88	3.05
	8	210	-44.74	0.76	0.74	1.77
	10	202	-53.98	0.61	0.58	5.15
	12	192	-59.64	0.43	0.45	5.93
	14	182	-73.25	0.25	0.28	9.73

3.1. Hysteresis, sensitivity and limit of detection (LOD) of the sensors

For hysteresis analysis, the sugar concentration is increased and then decreased across the full working range of the sensor in steps of 2 g/ml, and the visibility of the interference pattern is determined as presented in Figure 5. Overall, the concentration vs. visibility curves followed parabolic trends. However, two distinct linear regions can be identified: one in the lower concentration range (0-6 g/50 ml) and another in the higher concentration range (6-14 g/50 ml), which are used to determine the respective sensitivities and LODs. The parabolic and linear fitting functions and related parameters are listed in Table 2. The hysteresis values are 0.95%, 0.91%, and 2.63% of the maximum visibilities for the interference patterns of sucrose, glucose and fructose, respectively. Sensitivities are determined from the respective slope of the linear curve fitting and LOD is determined by: $LOD = 3(\frac{\delta}{S})$ [57], where, δ is the standard deviation of the intercept and S is the slope of the calibration curve. In the region-1, fructose offered the highest sensitivity of 0.0195 (g/50 ml)$^{-1}$, which was 6.09 times that of glucoseand 1.89 times that of sucrose. In the region-2, fructose again offered the highest sensitivity of 0.077 (g/50 ml)$^{-1}$, which was 3.56 times that of glucose and 2.41 times that of sucrose. The LODs were also calculated from the fitting parameters in both regions for each sugar sample. In the region-1, sucrose offered the lowest LOD of 0.0021 g/ml, which was 2.76-fold that of glucose and 1.71-fold that of fructose. In the region-2, sucrose again offered the lowest LOD of 0.0036 g/ml, which was 1.30-fold that of glucose and 1.18-fold that of fructose. Table 3 compares the sensitivities and LODs of the interferometric polarimeter in the two linear regions with those of the our recently reported PLRA polarimeter [44]. It can be seen that the interferometric polarimeter offered 18.29 times and 16.11 times improved LODs than the PLRA polarimeter in the regions 1 and 2, respectively.

Table 2
Curve fitting parameters of parabolic and linear functions applied to the data points of Figure 5. Only the increasing concertation curve fitting parameters are listed here

Sugar type	Polynomial fit ($y = ax^2 + bx + c$)			Linear fit ($y = mx + p$)			
				Region-1 (0 – 6 g/50 ml)		Region-2 (6 – 14 g/50 ml)	
	a	b	c	m	p	m	p
Sucrose	-0.0015	-0.0020	0.9716	-0.0103	0.9759	-0.0320	1.1070

Glucose	-0.0013	0.0041	0.9759	-0.0032	0.9799	-0.0216	1.0920
Fructose	-0.0040	0.0047	0.9641	-0.0195	0.9790	-0.0216	1.3431

Table 3
Sensitivities and LODs of the individual sugar samples and their comparison with the PLRA polarimeter

Sugar type	Region-1 (0 – 6 g/50 ml)		Region-2 (6 – 14 g/50 ml)		PLRA Polarimeter [44]	
	Sensitivity (g/50 ml)	LOD (g/ml)	Sensitivity (g/50 ml)	LOD (g/ml)	Sensitivity (deg ml g^{-1})	LOD (g/ml)
Sucrose	0.0103	0.0021	0.032	0.0036	163.41	0.0407
Glucose	0.0032	0.0058	0.0216	0.0046	122.06	0.0948
Fructose	0.0195	0.0036	0.0770	0.0042	272.84	0.0689

Figure 5
Repeatability and hysteresis analysis of the proposed interferometric polarimeter for one full cycle of the increasing and decreasing concentrations for (a) sucrose, (b) glucose and (c) fructose. Each parabolic curve can be divided into two linear regions: 0 – 6 g/50 ml and 6 – 14 g/50 ml, as shown in the inset of the plots

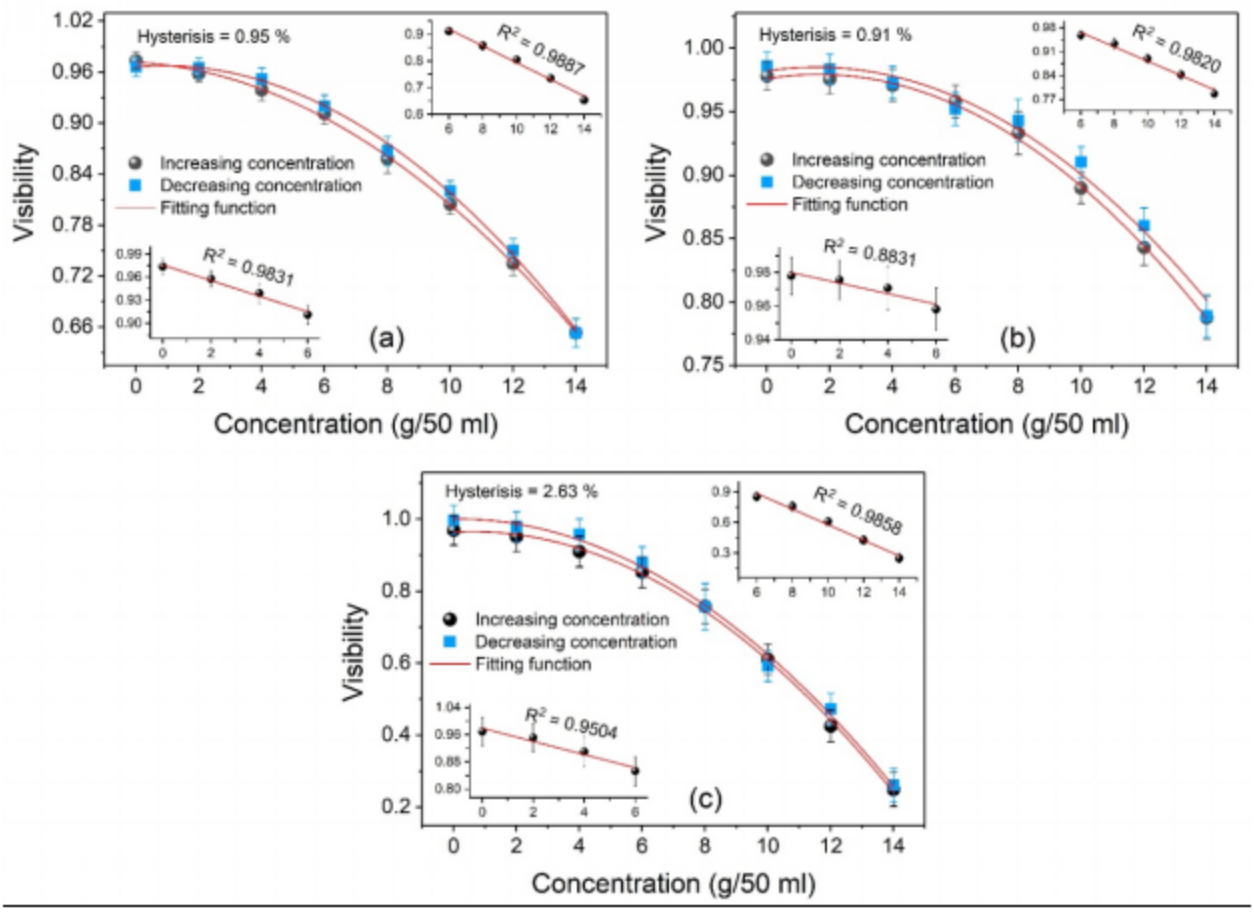

4. Conclusion

An interferometric-polarimeter based sugar sensor has been developed and demonstrated. Concentration of the sugar solution was determined from the visibility of Mach-Zehnder interference pattern. The visibility is found to be directly affected by concentration of the sugar solution due to its optical rotation and irradiance of the laser beam passing through the sample. The sensor offered a parabolic response for interference pattern visibility variation with change in the sugar solution concentration. Two distinct linear regions 0 – 6 g/50 ml and 6 – 14 g/50 ml are identified for sensitivity and LOD calculation. In the region-1, fructose had highest sensitivity of 0.0195 $(g/50\ ml)^{-1}$, which was 6.09 times that of glucose and 1.89times that of sucrose. Also, in the region-2, fructose showed sensitivity of 0.077 $(g/50\ ml)^{-1}$, which was 3.56 times and 2.41 times higher than those of glucose and that of sucrose, respectively. In the region-1, sucrose offered the lowest LOD of 0.0021 g/ml, which was 2.76-fold better than that of glucose and 1.71-fold that of fructose. In the region-2, sucrose had the lowest LOD of 0.0036 g/ml, which was 1.30-fold improved than that of glucose and 1.18-fold that of fructose. For hysteresis analysis, repeatability response is observed in one full cycle of increasing and decreasing concentrations of the sugar solutions. An average deviation of ±0.011, ±0.010 and ±0.029 is observed in the visibilities detected in increasing and decreasing concentrations of sucrose, glucose and fructose. This confirms the acceptable precision and hysteresis free response of the sensor. Visibilities of the interference patterns were also confirmed from the irradiance and optical rotation of the sample beams with respect to the reference beam at different concentrations of sugar solutions. An average deviation of 1.75%, 1.72%, and 4.24% is found in the visibilities calculated by the two different optical schemes for sucrose, glucose and fructose, respectively. Thus, the performance of the novel polarization-sensitive interferometric scheme was cross-checked and found to be satisfactory.

Ethical Statement

This study does not contain any studies with human or animal subjects performed by any of the authors.

Conflicts of Interest

The authors declare that they have no conflicts of interest to this work.

Data Availability Statement

Data are available from the corresponding author upon reasonable request.

Author Contribution Statement

Rahim Ullah: Conceptualization, Methodology, Validation, Investigation, Writing - original draft, Writing - review & editing, Visualization. **Raheem Dad Khan**: Methodology, Investigation. **Ghazanfar Hussain**: Conceptualization. **Rahat Ullah**: Validation, Investigation, Writing - review & editing. **Muhammad Faisal**: Methodology, Validation.

References

[1] Magwaza, L. S., & Opara, U. L. (2015). Analytical methods for determination of sugars and sweetness of horticultural products—A review. *Scientia Horticulturae, 184*, 179–192. https://doi.org/10.1016/j.scienta.2015.01.001

[2] de Souza, V. R., Pereira, P. A. P., Pinheiro, A. C. M., Bolini, H. M. A., Borges, S. V., & Queiroz, F. (2013). Analysis of various sweeteners in low-sugar mixed fruit jam: Equivalent sweetness, time-intensity analysis and acceptance test. *International Journal of Food Science & Technology, 48*(7), 1541–1548. https://doi.org/10.1111/ijfs.12123

[3] Singh, P., Ban, Y. G., Kashyap, L., Siraree, A., & Singh, J. (2020). Sugar and sugar substitutes: Recent developments and future prospects. In N. Mohan & P. Singh (Eds.), *Sugar and sugar derivatives: Changing consumer preferences* (pp. 39–75). Springer. https://doi.org/10.1007/978-981-15-6663-9_4

[4] Das, S., Ng, W. K., & Tan, R. B. H. (2014). Sucrose ester stabilized solid lipid nanoparticles and nanostructured lipid carriers: I. Effect of formulation variables on the physicochemical properties, drug release and stability of clotrimazole-loaded nanoparticles. *Nanotechnology, 25*(10), 105101. https://doi.org/10.1088/0957-4484/25/10/105101

[5] Kadajji, V. G., & Betageri, G. V. (2011). Water soluble polymers for pharmaceutical applications. *Polymers, 3*(4), 1972–2009. https://doi.org/10.3390/polym3041972

[6] Naseema, A., Kovooru, L., Behera, A. K., Kumar, K. P. P., & Srivastava, P. (2021). A critical review of synthesis procedures, applications and future potential of nanoemulsions. *Advances in Colloid and Interface Science, 287*, 102318. https://doi.org/10.1016/j.cis.2020.102318

[7] Szűts, A., & Szabó-Révész, P. (2012). Sucrose esters as natural surfactants in drug delivery systems—A mini-review. *International Journal of Pharmaceutics, 433*(1–2), 1–9. https://doi.org/10.1016/j.ijpharm.2012.04.076
[8] Bernal, P., & Llamas, M. A. (2012). Promising biotechnological applications of antibiofilm exopolysaccharides. *Microbial Biotechnology, 5*(6), 670–673. https://doi.org/10.1111/j.1751-7915.2012.00359.x
[9] Evans, G. G., & Furlong, J. (2011). *Environmental biotechnology: Theory and application*. USA: Wiley.
[10] Patel, S., & Goyal, A. (2011). Functional oligosaccharides: Production, properties and applications. *World Journal of Microbiology and Biotechnology, 27*(5), 1119–1128. https://doi.org/10.1007/s11274-010-0558-5
[11] Bruen, D., Delaney, C., Florea, L., & Diamond, D. (2017). Glucose sensing for diabetes monitoring: Recent developments. *Sensors, 17*(8), 1866. https://doi.org/10.3390/s17081866
[12] Chen, Q., Zhao, Y., & Liu, Y. (2021). Current development in wearable glucose meters. *Chinese Chemical Letters, 32*(12), 3705–3717. https://doi.org/10.1016/j.cclet.2021.05.043
[13] Jang, S., Wang, Y., & Jang, A. (2022). Review of emerging approaches utilizing alternative physiological human body fluids in non- or minimally invasive glucose monitoring. In K. K. Sadasivuni, J. J. Cabibihan, A. K. A. M. Al-Ali & R. A. Malik (Eds.), *Advanced bioscience and biosystems for detection and management of diabetes* (pp. 9 – 26). Springer. https://doi.org/10.1007/978-3-030-99728-1_2
[14] Mandpe, P., Prabhakar, B., Gupta, H., & Shende, P. (2020). Glucose oxidase-based biosensor for glucose detection from biological fluids. *Sensor Review, 40*(4), 497–511. https://doi.org/10.1108/SR-01-2019-0017
[15] Park, H., Park, W., & Lee, C. H. (2021). Electrochemically active materials and wearable biosensors for the in situ analysis of body fluids for human healthcare. *NPG Asia Materials, 13*(1), 23. https://doi.org/10.1038/s41427-020-00280-x
[16] Senf, B., Yeo, W. H., & Kim, J. H. (2020). Recent advances in portable biosensors for biomarker detection in body fluids. *Biosensors, 10*(9), 127. https://doi.org/10.3390/bios10090127
[17] Bell, S. J., & Sears, B. (2003). Low-glycemic-load diets: Impact on obesity and chronic diseases. *Critical Reviews in Food Science and Nutrition, 43*(4), 357–377. https://doi.org/10.1080/10408690390826554
[18] Aronne, G., & Malara, P. (2019). Fiber-optic refractometer for in vivo sugar concentration measurements of low-nectar-producing flowers. *New Phytologist, 224*(2), 987–993. https://doi.org/10.1111/nph.16084
[19] Rao, B. S., Nurfaiz, M., & Hashim, U. (2013). Quantitative measurement of sugar concentration using in house fabricated microgap biosensor. In *RSM 2013 IEEE Regional Symposium on Micro and Nanoelectronics*, 54 – 57. https://doi.org/10.1109/RSM.2013.6706471
[20] Borji, A., Borji, F., & Jourani, A. (2017). A new method for the determination of sucrose concentration in a pure and impure system: Spectrophotometric method. *International Journal of Analytical Chemistry, 2017*(1), 8214120. https://doi.org/10.1155/2017/8214120
[21] Rondonuwu, F. S., Setiawan, A., & Karwur, F. F. (2019). Determination of glucose concentration in aqueous solution using FT NIR spectroscopy. *Journal of Physics: Conference Series, 1307*(1), 012019. https://doi.org/10.1088/1742-6596/1307/1/012019
[22] Suhandy, D., Suzuki, T., Ogawa, Y., Kondo, N., Ishihara, T., & Takemoto, Y. (2011). A quantitative study for determination of sugar concentration using attenuated total reflectance terahertz (ATR-THz) spectroscopy. In *Sensing for Agriculture and Food Quality and Safety III, 8027*, 802705. https://doi.org/10.1117/12.886183
[23] Suhandy, D., Suzuki, T., Ogawa, Y., Kondo, N., Naito, H., Ishihara, T., ..., & Liu, W. (2012). A quantitative study for determination of glucose concentration using attenuated total reflectance terahertz (ATR-THz) spectroscopy. *Engineering in Agriculture, Environment and Food, 5*(3), 90–95. https://doi.org/10.11165/eaef.5.90
[24] Aguila Rodriguez, G., Arias Duque, N. P., Gonzalez Sanchez, B. E., Sandoval Gonzalez, O. O., Giraldo Osorio, O. H., Trujillo Romero, C. J., ..., & de Jesus Agustin Flores Cuautle, J. (2019). Sugar concentration measurement system using radiofrequency sensor. *Sensors, 19*(10), 2354. https://doi.org/10.3390/s19102354
[25] Lee, D. K., Kang, J. H., Lee, J. S., Kim, H. S., Kim, C., Hun Kim, J., ..., & Seo, M. (2015). Highly sensitive and selective sugar detection by terahertz nano-antennas. *Scientific Reports, 5*(1), 15459. https://doi.org/10.1038/srep15459
[26] Fan, Y., Deng, X., Wang, Q., & Wang, W. (2010). Testing glucose concentration in aqueous solution based on microwave cavity perturbation technique. In *3rd International Conference on Biomedical Engineering and Informatics*, 1046 – 1049. https://doi.org/10.1109/BMEI.2010.5639744
[27] McNichols, R. J., & Cote, G. L. (2000). Optical glucose sensing in biological fluids: An overview. *Journal of Biomedical Optics, 5*(1). https://doi.org/10.1117/1.429962
[28] Kabilan, S., Marshall, A. J., Sartain, F. K., Lee, M. C., Hussain, A., Yang, X., ..., & Lowe, C. R. (2005). Holographic glucose sensors. *Biosensors and Bioelectronics, 20*(8), 1602–1610. https://doi.org/10.1016/j.bios.2004.07.005
[29] Worsley, G. J., Tourniaire, G. A., Medlock, K. E. S., Sartain, F. K., Harmer, H. E., Thatcher, M., ..., & Pritchard, J. (2007). Continuous blood glucose monitoring with a thin-film optical sensor. *Clinical Chemistry, 53*(10), 1820 – 1826. https://doi.org/10.1373/clinchem.2007.091629
[30] Scampicchio, M., Arecchi, A., & Mannino, S. (2009). Optical nanoprobes based on gold nanoparticles for sugar sensing. *Nanotechnology, 20*(13), 135501. https://doi.org/10.1088/0957-4484/20/13/135501
[31] Mahajan, S., Trivedi, V., Chhaniwal, V., Prajapati, M., Zalevsky, Z., Javidi, B., & Anand, A. (2015). Measurement of concentration of sugar in solutions with laser speckle decorrelation. In *Optical Measurement Systems for Industrial Inspection IX, 9525*, 775-780. https://doi.org/10.1117/12.2184698
[32] Firdous, S., & Ikram, M. (2005). Polarized mueller matrix analytical model for glucose measurement in vitro. *Turkish*

Journal of Medical Sciences, 35(3), 3.
[33] Elsherif, M., Hassan, M. U., Yetisen, A. K., & Butt, H. (2018). Wearable contact lens biosensors for continuous glucose monitoring using smartphones. *ACS Nano, 12*(6), 5452–5462. https://doi.org/10.1021/acsnano.8b00829
[34] Cameron, B. D. (2007). *Noninvasive birefringence compensated sensing polarimeter* (United States Patent US7245952B2). Google Patents. https://patents.google.com/patent/US7245952B2/en
[35] Flores, J. L., Montoya, M., Garcia-Torales, G., & Alvarez, A. G. (2005). Polarimeter with linear response for measuring optical activity in organic compounds. In *Novel Optical Systems Design and Optimization VIII, 5875*, 58750U. https://doi.org/10.1117/12.617975
[36] Kothari, N., Jafarpour, A., Trebino, R., Thaler, T. L., & Bommarius, A. S. (2008). Astrobiological polarimeter. *Astrobiology, 8*(6), 1061–1069. https://doi.org/10.1089/ast.2007.0151
[37] Mohd Zain, M. N., Musa, A., Hisham, M. H., Laili, A. R., & Yusof, Z. M. (2014). Photon counting polarimetry measurement towards non-invasive biomedical glucose monitoring. In *IEEE 5th International Conference on Photonics*, 156–158. https://doi.org/10.1109/ICP.2014.7002364
[38] Calixto, S., Martinez-Ponce, G., Garnica, G., & Figueroa-Gerstenmaier, S. (2017). A wavefront division polarimeter for the measurements of solute concentrations in solutions. *Sensors, 17*(12), 2844. https://doi.org/10.3390/s17122844
[39] Alonso-González, A., López-Martínez, C., Papathanassiou, K. P., & Hajnsek, I. (2020). Polarimetric SAR time series change analysis over agricultural areas. *IEEE Transactions on Geoscience and Remote Sensing, 58*(10), 7317 – 7330. https://doi.org/10.1109/TGRS.2020.2981929
[40] Gambelli, L. (2017). Milk and its sugar-lactose: A picture of evaluation methodologies. *Beverages, 3*(3), 35. https://doi.org/10.3390/beverages3030035
[41] Iwuozor, K. O., Anyanwu, V. U., Olaniyi, B. O., Mbamalu, P. S., & Adeniyi, A. G. (2022). Adulteration of sugar: A growing global menace. *Sugar Tech, 24*(3), 914–919. https://doi.org/10.1007/s12355-022-01122-6
[42] Löw, J., Ullmann, T., & Conrad, C. (2021). The impact of phenological developments on interferometric and polarimetric crop signatures derived from Sentinel-1: Examples from the DEMMIN Study Site (Germany). *Remote Sensing, 13*(15), 2951. https://doi.org/10.3390/rs13152951
[43] Pirnstill, C. W., Malik, B. H., Gresham, V. C., & Coté, G. L. (2012). In vivo glucose monitoring using dual-wavelength polarimetry to overcome corneal birefringence in the presence of motion. *Diabetes Technology & Therapeutics, 14*(9), 819–827. https://doi.org/10.1089/dia.2012.0070
[44] Ullah, R., Faisal, M., & Ullah, R. (2023). Polarimetric and fluorescence spectroscopic based classification of mono and disaccharide solutions. *Spectrochimica Acta Part A: Molecular and Biomolecular Spectroscopy, 293*, 122490. https://doi.org/10.1016/j.saa.2023.122490
[45] de Almeida, F. S., Rocha, A. C. P., Lima, S. M., & Andrade, L. H. C. (2018). Spectral refractive index technique for monitoring the beer mashing process. *Applied Optics, 57*(16), 4672–4676. https://doi.org/10.1364/AO.57.004672
[46] Chen, M., Geiser, M., Truffer, F., & Song, C. (2012). Miniature interferometer for refractive index measurement in microfluidic chip. In *Optics in Health Care and Biomedical Optics V, 8553*, 85532Z. https://doi.org/10.1117/12.999280
[47] Chen, M. H., Geiser, M., Truffer, F., & Song, C. L. (2013). Development of interferometer for refractive index measurement of aqueous solution in a microfluidic chip. *Laser Physics Letters, 10*(4), 045701. https://doi.org/10.1088/1612-2011/10/4/045701
[48] Kachiraju, S. R., & Gregory, D. A. (2012). Determining the refractive index of liquids using a modified Michelson interferometer. *Optics & Laser Technology, 44*(8), 2361–2365. https://doi.org/10.1016/j.optlastec.2012.04.020
[49] Kussrow, A., Kaltgrad, E., Wolfenden, M. L., Cloninger, M. J., Finn, M. G., & Bornhop, D. J. (2009). Measurement of monovalent and polyvalent carbohydrate-lectin binding by back-scattering interferometry. *Analytical Chemistry, 81*(12), 4889–4897. https://doi.org/10.1021/ac900569c
[50] Kussrow, A., Enders, C. S., & Bornhop, D. J. (2012). Interferometric methods for label-free molecular interaction studies. *Analytical Chemistry, 84*(2), 779–792. https://doi.org/10.1021/ac202812h
[51] Meng, H., Shen, W., Zhang, G., Wu, X., Wang, W., Tan, C., & Huang, X. (2011). Michelson interferometer-based fiber-optic sensing of liquid refractive index. *Sensors and Actuators B: Chemical, 160*(1), 720 – 723. https://doi.org/10.1016/j.snb.2011.08.054
[52] Wąsik, S., Arabski, M., Dworecki, K., Janoska, J., Semaniak, J., Szary, K., & Ślęzak, A. (2014). Laser interferometric analysis of glucose and sucrose diffusion in agarose gel. *General Physiology and Biophysics, 33*(4), 383 – 391. https://doi.org/10.4149/gpb_2014016
[53] Ullah, R., Khan, R. Y. M., & Faisal, M. (2022). A review of optical interferometry techniques for quantitative determination of optically active materials in a solution. In M. Bhowmick (Ed.), *Optical interferometry—A multidisciplinary technique in science and engineering*, (pp. 5). IntechOpen. https://doi.org/10.5772/intechopen.104937
[54] Pisano, A. (2021). Light, air pollution, and pulse oximetry: The Beer–Lambert Law. In A. Pisano (Ed.), *Physics for anesthesiologists and intensivists: From daily life to clinical practice* (pp. 187–199). Springer. https://doi.org/10.1007/978-3-030-72047-6_16
[55] Ymeti, A., Kanger, J. S., Greve, J., Lambeck, P. V., Wijn, R., & Heideman, R. G. (2003). Realization of a multichannel integrated Young interferometer chemical sensor. *Applied Optics, 42*(28), 5649–5660. https://doi.org/10.1364/AO.42.005649
[56] Goraieb, K., Alexandre, T. L., & Bueno, M. I. M. S. (2007). X-ray spectrometry and chemometrics in sugar classification,

correlation with degree of sweetness and specific rotation of polarized light. *Analytica Chimica Acta, 595*(1–2), 170–175. https://doi.org/10.1016/j.aca.2007.04.025

[57] Ullah, R., Rasheed, M. A., Abbas, S., Rehman, K., Shah, A., Ullah, K., ..., & Ali, G. (2022). Electrochemical sensing of H_2O_2 using cobalt oxide modified TiO_2 nanotubes. *Current Applied Physics, 38*, 40 – 48. https://doi.org/10.1016/j.cap.2022.02.008

How to Cite:

Ullah, R., Khan, R. D., Hussain, G., Ullah, R., & Faisal, M. (2024). Design and Demonstration of a Novel Interferometric Polarimeter for Quantitative Determination of Sugars in a Solution. *Journal of Optics and Photonics Research*. https://doi.org/10.47852/bonviewJOPR42022890